

In Vivo OXPHOS Measurement by Magnetic Resonance Imaging in Metabolic Myopathy

Catherine DeBrosse¹, Ravi Prakash Reddy Nanga¹, Neil Wilson¹, Kevin D'Aquila¹, Mark Elliott¹, Hari Hariharan¹, Felicia Yan², Leat Perez², Sara Nguyen², Elizabeth McCormick³, Marni Falk^{3,4}, Shana McCormack^{2,4}, and Ravinder Reddy¹

¹Center for Magnetic Resonance and Optical Imaging, Department of Radiology, University of Pennsylvania, Philadelphia, Pennsylvania, United States, ²Division of Endocrinology and Diabetes, The Children's Hospital of Philadelphia, Philadelphia, PA, United States, ³Division of Human Genetics, The Children's Hospital of Philadelphia, Philadelphia, PA, United States, ⁴Perelman School of Medicine, University of Pennsylvania, Philadelphia, PA, United States

Introduction: During exercise, skeletal muscle utilizes energy in the form of ATP, generated by mitochondria through oxidative phosphorylation (OXPHOS)¹. Phosphocreatine (PCr), serves as a “reserve” of ATP. During exercise, PCr is converted into creatine (Cr), with simultaneous conversion of ADP to ATP. After exercise, the rate at which PCr is re-synthesized occurs in proportion to OXPHOS⁴. Patients with metabolic myopathies often experience exercise intolerance due to defects in OXPHOS². Currently, OXPHOS capacity is measured using ³¹P magnetic resonance spectroscopy (MRS)³. ³¹P MRS studies have shown a prolonged PCr recovery time in patients with mitochondrial diseases⁵. Though ³¹P MRS has provided key insight into PCr recovery kinetics, it lacks spatial resolution and sensitivity. Recently, a magnetic resonance imaging (MRI) method has been developed to address these shortcomings: creatine chemical exchange saturation transfer (CrCEST)⁶. This technique images free creatine (Cr) in skeletal muscle, with high spatial resolution that allows individual muscle groups to be distinguished. Previous CrCEST studies have shown that the post-exercise Cr decrease can be imaged, and corresponds to the PCr recovery observed with ³¹P MRS^{6,7}. In this study, we demonstrate the ability of CrCEST to show differences in resting Cr levels and post-exercise recovery rates in patients with metabolic myopathies vs. healthy subjects.

Methods: CrCEST images were acquired on 5 patients with metabolic myopathies on a 7T whole body scanner (Siemens Medical Systems, Erlangen, Germany). All patient studies were performed under an approved Institutional Review Board protocol of the University of Pennsylvania (NCT02154711). Imaging experiments were performed using a 28-channel ¹H knee coil. CrCEST imaging parameters: saturation pulse = 500 ms, B1_{rms} = 123 Hz (2.9 µT), slice thickness = 10 mm, flip angle = 10°, TR = 6.0 ms, TE = 2.9 ms, field of view = 140 x 140 mm², matrix size = 128 x 128. Four baseline images were acquired over 2 minutes, followed by 2 minutes of mild plantar flexion exercise, and 8 minutes of post-exercise imaging (16 images). Exercise was performed in the magnet using an MR-compatible, pneumatically controlled foot pedal. Image processing was performed using in-house MATLAB scripts. B₀ and B₁ maps were used to generate corrected CEST images as described for previous studies⁶. CrCEST contrast was computed by subtracting the normalized magnetization signal at the Cr proton frequency ($\Delta\omega = +1.8$ ppm), from the magnetization at the corresponding reference frequency on the opposite side of the water resonance ($-\Delta\omega$), according to the following equation⁸ : $CEST_{asym}(\Delta\omega) = (M_{sat}(-\Delta\omega) - M_{sat}(+\Delta\omega)) / M_{sat}(-\Delta\omega)$. CEST_{asym} changes in individual muscle groups pre- and post-exercise were determined by overlaying CEST_{asym} maps onto manually segmented anatomic images. Maps were scaled from 0-22% CrCEST_{asym}. ³¹P MRS was performed with a 7-cm diameter ¹H/³¹P dual tuned surface coil using an unlocalized free induction decay (fid) sequence: number of points = 512, averages = 5, and TR = 3.0 s. ³¹P MRS Spectra were phased and baseline corrected and fitted using nonlinear least squares method with Lorentzian functions.

Results and Discussion: Five patients (2 males, 3 females: ages 21-59yrs) with metabolic myopathies were imaged using

CrCEST. Results were compared to historical control data from previously published healthy subjects⁶ (4 males, 3 females: ages 19-30 yrs) using the same exercise paradigm. CrCEST_{asym} was evaluated in four muscles of the lower leg compartment: anterior tibialis (AT), soleus (S), medial gastrocnemius (MG), and lateral gastrocnemius (LG). Plantar flexion exercise was used to induce PCr and Cr changes in the gastrocnemius muscles.

Representative CrCEST_{asym} maps are shown for one healthy subject (Fig 1) and one patient exhibiting classic mitochondrial encephalomyopathy, lactic acidosis, and stroke-like episodes (MELAS) not taking exogenous creatine (Fig 2). The CEST maps show that the MELAS patient has lower baseline creatine values than the healthy subject. Group analysis shows that, on average, the baseline value of CrCEST_{asym} (pre-exercise) for individual muscle groups was lower in patients than healthy subjects (Fig 3). This finding was statistically significant for 3 muscle groups ($p < 0.01$ AT, S; $p < 0.05$, MG; $p < 0.1$ LG). Low levels of total creatine in muscle tissue are thought to be from reduced transport into muscles of affected patients⁹.

Mitochondrial function is typically measured post-exercise by calculating the recovery time of PCr. With CrCEST, we determined the Cr increase and subsequent recovery rate post-exercise for individual muscle groups. PCr recovery time constants were also calculated (Fig 4). The overall trend for PCr and Cr recovery shows that in the patient population, recovery took ~1.6x as long as in healthy subjects. Due to inter-subject variability, these rates should be examined in a larger patient population to improve statistical power.

The advantages of CrCEST over ³¹P MRS are especially suited for study of metabolic disorders. Often, patients with mitochondrial impairment have regional tissue differences in muscle capacity¹⁰. With the spatial resolution provided by CrCEST, we can assess creatine levels in individual muscle groups. As described previously⁶, this technique shows that people may be exercising muscles other than the MG/LG, which should be activated by plantar flexion. For patient populations that have been studied using plantar flexion and ³¹P MRS, there is a possibility that data was excluded as no PCr changes were detected after exercise, perhaps because subjects were using other than MG/LG. With CrCEST, creatine recovery rates can be determined for each muscle group, providing better insight into which muscles may be utilized.

Conclusion: CrCEST imaging shows differences in creatine metabolism between healthy subjects and patients with metabolic myopathies. Patients had longer CrCEST return to baseline times after exercise, corresponding with delayed PCr recovery times. CrCEST provides additional spatial information regarding utilized muscle groups compared to standard ³¹P MRS in patients with impaired metabolism. Further studies in a larger cohort of patients with metabolic disorders and age-matched healthy control subjects are in progress.

References: [1] Chance et al. *J Biol Chem* 217: 409-427 (1955) [2] Kent-Braun et al. *J Appl Physiol* 89:1072-1078 (1985) [3] DiMauro *Current opinion in rheumatology* 18: 636-641 (2006) [4] Hoult et al. *Nature* 252:285-287 (1974) [5] Chance et al. *Biochimica et biophysica acta* 1271:7-14 (1995) [6] Kogan et al. *Magnetic resonance in medicine* 71:164-172 (2014) [7] Kogan et al. *Journal of magnetic resonance imaging* 40: 596-602 (2014) [8] Haris et al. *NeuroImage* 54: 2079-85 (2010) [9] Tarnopolsky et al. *Muscle Nerve* 22:1228-1233 (1999) [10] Horiuchi et al. *Experimental physiology* 99: 348-358 (2013)

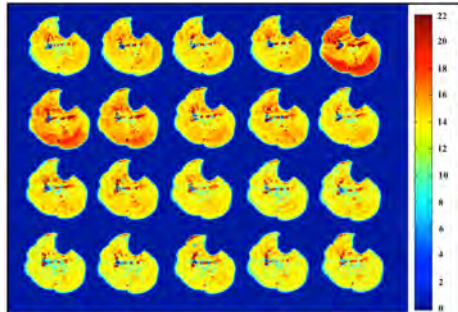


Figure 1: CrCEST_{asym} map of healthy subject's calf muscle

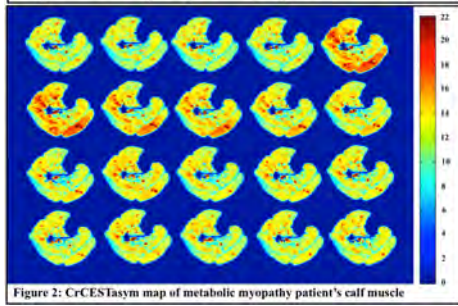


Figure 2: CrCEST_{asym} map of metabolic myopathy patient's calf muscle

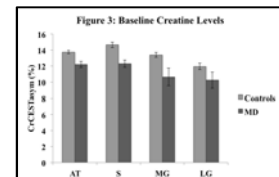


Figure 3: Baseline Creatine Levels

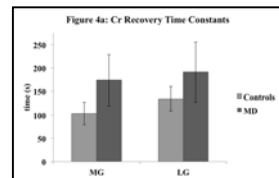


Figure 4a: Cr Recovery Time Constants

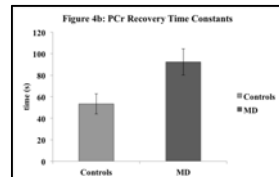


Figure 4b: PCr Recovery Time Constants